Advanced Lab: Measurement of the mean muon lifetime

Deniz Defne Köksal, Leon Fischer*
Humboldt Universität zu Berlin, Supervisor: Dr. Marzieh Bahmani
(Dated: December 20, 2023)

In this paper, we present our measurement of the mean muon lifetime of $\tau_\mu = 2.24 \pm 0.09\mu s$. The chosen experimental setup used cosmic radiation as a muon source. The incoming muons were slowed down to a static state passing through matter resulting them to undergo a decay. Both the muons and the decay products were detected via scintillation detectors.

I. INTRODUCTION

According to the standard model of particle physics, muons μ^- are part of the second generation of matter as unstable leptons, meaning as unstable elementary particles, that do not interact strongly.
Their mean lifetime can be experimentially determined using the flux of muons μ^- and antimuons μ^+ at sea level, that are originating from cosmic showers initiated by high energy cosmic rays and atoms interacting in the upper atmosphere.
These muons and antimuons continue to decay weakly, mediated by the W^-, W^+ boson respectively.
Taking all the conservation laws into consideration, such as electric charge, lepton number and the lepton family number conservation, the following decays are the only allowed ones in the first order:

$$\mu^- \to e^- + \bar{\nu_e} + \nu_\mu \tag{1}$$
$$\mu^+ \to e^+ + \nu_e + \bar{\nu_\mu} \tag{2}$$

The associated Feynman diagram for the negatively charged muon decay is as follows:

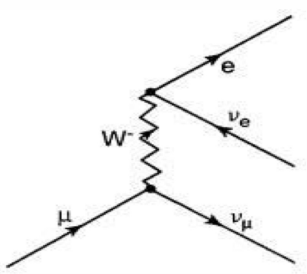

Figure 1. Feynman diagram for the decay of negatively charged muons[2]

Higher order processes are negligible, so we can assume the total decay rate, which is equal to the decay width if one sets $\hbar = 1$, to be determined by the first order processes allowed for muons and antimuons respectively.

The decay rate (per muon) can be written as:

$$\Gamma = \frac{G_F^2 m_\mu^5}{192\pi^3} \tag{3}$$

where G_F denotes the coupling constant and m_μ the muon mass. Since this is a constant decay rate per particle, an initial number of muons will decay exponentially, yielding the relation:

$$\Gamma = \frac{1}{\tau_\mu} \tag{4}$$

As stated above, the exponential decay law is the right way of modeling free muon decay. However, a negatively charged muon can also be captured by an atom while moving through matter, in this case leading to an effective lifetime[1]:

$$\frac{1}{\tau_{\text{eff}}} = \frac{Q}{\tau_\mu} + \Lambda_C \tag{5}$$

where Q denotes the Huff-Factor and Λ_C the capture rate. Both are material specific quantities.
In the case of cosmic muons moving through a material, we have both muons and antimuons decaying, meaning the number of decays in a time interval of length dt in a given material should be expressed with the modified exponential law, where we also consider the atomic capture[2]:

$$-\mathrm{d}N(t) = N_{\mu^+}\left(\frac{1}{f}\cdot\frac{1}{\tau_{\text{eff}}}e^{-t/\tau_{\text{eff}}} + \frac{1}{\tau_\mu}\cdot e^{-t/\tau_\mu}\right)\mathrm{d}t \tag{6}$$

where $f = N_{\mu^+}/N_{\mu^-}$ is the ratio of antimuons to muons.

II. EXPERIMENTAL SETUP

As shown in Figure 2, the muons and other possible incoming particles first encounter the lead absorber. Muons pass through, whereas other particles are in good approximation shielded. They then get detected by the scintillators SC1 and SC2, moving on to the aluminum

* Correspondence email addresses: koeksald@physik.hu-berlin.de, fiserlef@hu-berlin.de

[1] 1, Equ.(11), p.5.
[2] 1, Equ.(14), p.6.

block, where they decay. The electrons or positrons that leave the aluminum block get detected by either scintillator SC2 or SC3. The neutrinos can not be detected by a scintillator, since they only interact weakly and therefore would not cause a noticeable excitation in the scintillator material used.

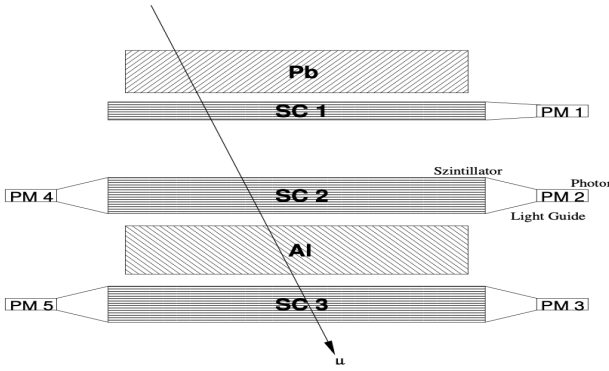

Figure 2. Detector arrangement for measuring the muon lifetime[1]

All scintillators are coupled to photomultipliers via lightguides. The signals coming from the photomultipliers travel through a circuit of NIM modules, and the final spectrum was recorded with a computer program.

III. PREPARATORY MEASUREMENTS

A multitude of preparatory tasks were completed before performing the actual measurement.

A. Runtime behaviour of signals

As explained in IV, signals go through coincidence units, which introduce delay times to the runtime while processing the signal. In order to understand how much this systematic error influences the measurement, we used a oscilloscope to measure the delay time of a chosen coincidence unit. This was done by displaying the respective input signal relative to the output signal on a time scale. Guides were then used to measure Δt_c for three different coincidence units. This yielded $\Delta t_c = 14.53 \pm 0.32\,\text{ns}$. An exemplary screenshot of one delay measurement can be found below:

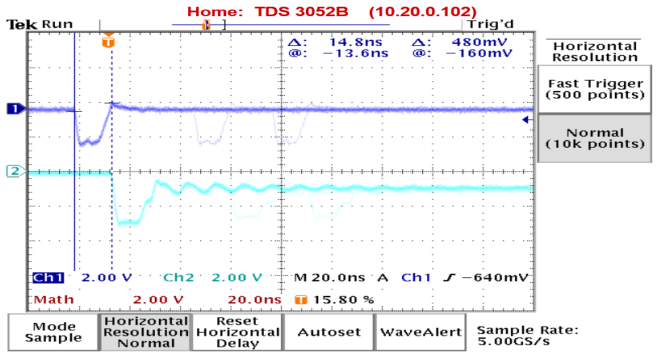

Figure 3. Screenshot of a coincidence unit delay time measurement using the oscilloscope

In addition to the delay of coincidence units, another delay is introduced to the runtime because of the cables themselves. The delay of the cable type RG58U[3] $\Delta t = 5.14\,\text{ns/m}$ leads to a delay of $\Delta t_s = 1.03\,\text{ns}$ for each short cable of 20 cm length and $\Delta t_l = 1.55\,\text{ns}$ for each long cable of 30 cm length used. Relevant to our measurement of τ_μ is only the difference in runtime of the signals leading to the START and STOP signals incident at the TAC. Compared to the START signal, one more coincidence unit and one more short cable was used to generate the STOP signal, leading to an added delay of $\Delta t = 15.56 \pm 0.32\,\text{ns}$ between the two. This delay has to be subtracted from our calculated value of τ_μ.

B. Event rates

To see that setting two photomultipliers in coincidence per scintillator serves as noise suppression, we firstly measured the event rates of each photomultiplier individually. Afterwards, event rates for PM2 ∧ PM4 and PM3 ∧ PM5 were measured, and additionally a couple more logical arrangements of signals. The event rates were counted using the quad scaler. For each arrangement, 4 measurements were carried out to calculate mean value and standard error. Some of the results relevant for further discussion can be found in the following table:

Signal	Count rate (1/s)
PM1	1339 ± 83
PM2	852 ± 59
PM4	1224 ± 16
PM3	1210 ± 50
PM5	952 ± 26
SC2	142 ± 10
SC3	157 ± 5

Table I. Count rates of different signals

[3] 3, p.264.

It can be seen that requiring a coincidence of PM2 ∧ PM4 or PM3 ∧ PM5 results in a loss of efficiency of 86% or 85% respectively. This indicates a high amount of noise (e.g. thermal noise in the photomultiplier tubes) that is cancelled by the use of coincidence units. Note that although no left-right-coincidence is required in SC1, the noise of SC1 is still suppressed, because a START signal also requires a signal in SC2.
All other measured rates were consistent with each other in the sense that specific opposing signal arrangements added up to a total rate consistent with the non-specific rate of the same arrangement (e.g. SC1 ∧ SC2 ¬ SC3 + SC1 ∧ SC2 ∧ SC3 = SC1 ∧ SC2). At the same time, the signals incident at the counters

C. Time calibration

The TAC-unit measures the time difference between its START and STOP signal indirectly. It converts the time difference into an amplitude of its output pulse, meaning longer time differences correspond to higher amplitudes. The ADC associates this pulse amplitude to a channel number, hence for determining a time difference one needs to know about the conversion of channel numbers into time of the ADC. The following circuit was used the determine said conversion.

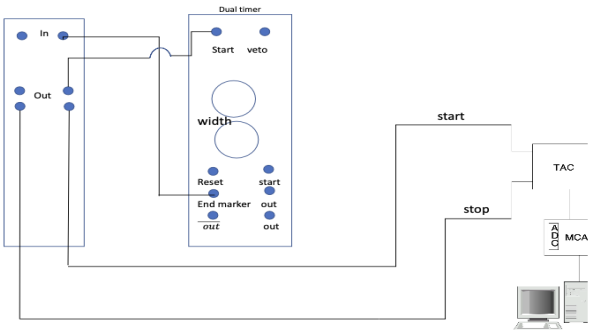

Figure 4. Time calibration circuit used to determine conversion of channel number to time[1]

Here a coincidence unit and a dual timer are used to generate, duplicate and delay pulses by a variable time difference. This time difference is then converted by TAC and ADC into a channel number as explained above. Various different delay times between 0.92 µs an 19.1 µs were set using the oscilloscope, since the dual timer had a non linear behaviour at the lower end, and then measured using the TAC and MCA. Each measurement was run for roughly one second, and 20 data points were taken in total. All measurements were entered in a single spectrum consisting of data pairs (channel number, entries). Each set delay time was then paired with the corresponding channel number to perform a linear fit on (time, channel number). Only the errors of the time values were taken into account here, but not those of the channel values, since the relative errors of the time values ($\mathcal{O}(5 \cdot 10^{-3})$ were greater than the relative errors of the channel numbers ($\mathcal{O}(1 \cdot 10^{-4})$. Time errors were calculated based on the assumption that the main cause of error during this measurement was the width of the signal displayed on the oscilloscope. We calculated the width of the signal by analysing the amounts of pixels it used on a screenshot of the oscilloscope screen and then converting pixels into time using the time scale set on the oscilloscope. Half of the width was then assumed as error of the measured time values, since any value within the width of the signal was considered correctly measured. This yielded an error of 54.4 ns. For all time delay values larger than 10 µs, the oscilloscope only displayed one digit after the decimal point, which is why the measurement error was rounded up to the same decimals. As displayed in figure 5, the delay measured in channel one corresponds to the amplitude of the TAC signal measured in channel two. One could say the horizontal distance between signals in channel one corresponds to a vertical distance between plateau and baseline in channel two. This relationship was directly observed while changing time delays.

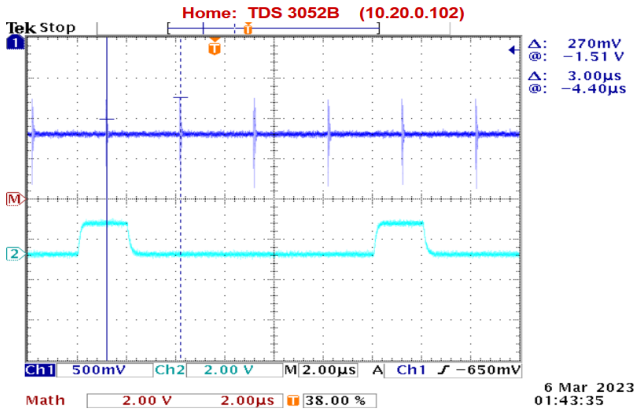

Figure 5. Screenshot of oscilloscope screen displaying a signal generated with 3.00 µs delay

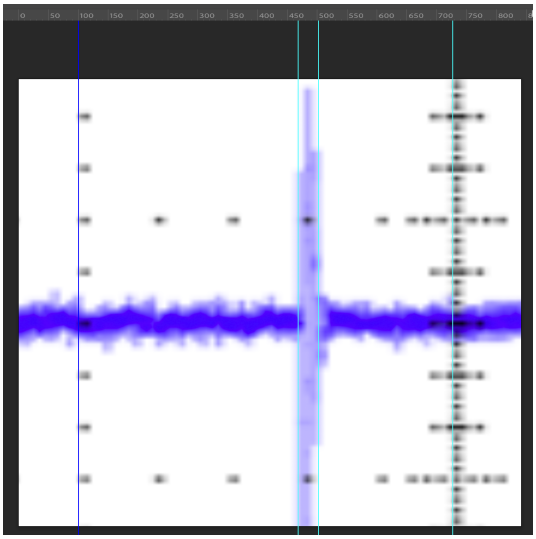

Figure 6. Pixel width measurement of the generated signal

The resulting data can be found in the table below:

Set delay time (µs)	Channel number
0.92 ± 0.06	185.00 ± 0.00
2.42 ± 0.06	499.00 ± 0.08
3.08 ± 0.06	634.00 ± 0.00
3.88 ± 0.06	804.00 ± 0.00
4.70 ± 0.06	962.00 ± 0.00
5.58 ± 0.06	1158.00 ± 0.00
6.60 ± 0.06	1368.72 ± 0.11
7.68 ± 0.06	1589.72 ± 0.13
8.68 ± 0.06	1789.00 ± 0.00
9.72 ± 0.06	2015.00 ± 0.16
10.6 ± 0.1	2217.00 ± 0.17
11.7 ± 0.1	2416.00 ± 0.20
12.5 ± 0.1	2604.00 ± 0.22
13.4 ± 0.1	2802.72 ± 0.14
14.2 ± 0.1	2973.27 ± 0.12
15.4 ± 0.1	3212.07 ± 0.13
16.3 ± 0.1	3393.92 ± 0.15
17.5 ± 0.1	3670.05 ± 0.15
18.2 ± 0.1	3775.48 ± 0.15

Table II. Data of the time calibration measurement

The plot of our time calibration data together with the linear fit funtion and the fit parameter values are shown in figure 7.

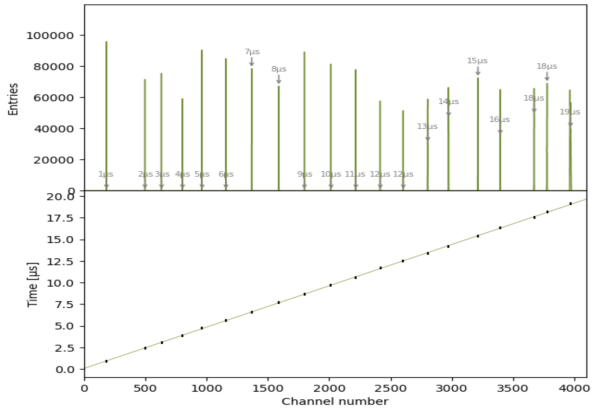

Figure 7. Time calibration spectrum with linear fit function $f(x) = m \cdot x + b$

Parameter	Value
m	4.786± 0.011 ns/channel number
b	0.046 ± 0.025 ns
χ^2/DoF	0.964444

Table III. Linear fit parameters for time calibration

IV. MUON LIFETIME MEASUREMENT

Figure 8 shows the circuit used to measure the mean lifetime of muons.

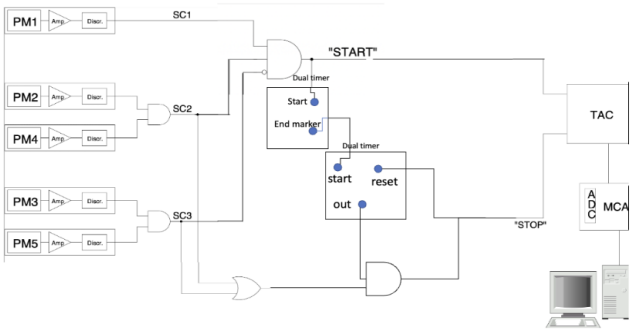

Figure 8. Muon lifetime measurement circuit[1]

The signals coming from the photomultipliers are first sent through an amplifier and then to a discriminator. Only the signals that are coincident in PM2 and PM4 are counted as signals from SC2, and similarly only the signals that are coincident in PM3 and PM5 are counted as signals form SC3. This has the purpose of noise suppression. The signals from SC1, SC2 and SC3 are then sent to another coincidence unit, which only sends an output signal if input signals from SC1 and SC2 but not SC3 are received. The output signal is split into two

signals via another coincidence unit, one of which starts the TAC timer, and the other starts the first dual timer. Additionally, the signals from SC2 and SC3 are also sent to a quad coincidence unit operating as a logical 'OR'. This means the unit sends an output signal if a signal from SC2 ∨ SC3 is received. The purpose of the first dual timer is further noise suppression. It creates a delay between the START signal and the STOP signal of 3 µs, and by doing so it blocks all signals from stopping the TAC timer that are received within the first 3 µs after the START signal was received. The output of the corresponding end marker is fed into the second dual timer, which creates a second interval of 17 µs. The output of the second dual timer is then fed into another coincidence unit, which only sends an output if the output signal from the 'OR' unit is coincident with the output of the second dual timer, i.e. if a signal from SC2 ∨ SC3 is detected within the time window of the second dual timer. The output of the coincidence unit is split via another coincidence unit into two, one of which sends a STOP signal to the TAC, the other resets the second timer, starting the process from the beginning. The TAC unit is connected to a MCA and an ADC. The raw data spectrum (channel number, entries) is accessed using the computer program MAESTRO. The measurement was running for roughly a day, after which the data was collected. The analysis of the data was performed using the provided Jupyter Notebook.

V. EVALUATION

The collected raw data (channel number, entries) was first converted to (time, entries) using the results from our calibration curve. Since the aim of this experiment was to determine the muon lifetime with an accuracy of 1%, the spectrum was then rebinned by adding every 20 adjacent channels into one. The choice of rebinning is justified, since a time difference between two adjacent channels corresponds to $\Delta t \approx 5\,\mathrm{ns}$ (III), meaning a channel number difference of 20 corresponds to $\Delta t \approx 5 \cdot 20\,\mathrm{ns} = 10^2\,\mathrm{ns} = 0.1\,\mu\mathrm{s}$. This is smaller than 1% of the literature value[4] of $\tau_\mu = 2.19703(4)\,\mu\mathrm{s}$. Rebinning was also started at channel 620, because it was the first channel with entries $\neq 0$, and endet with channel 3900, because it was the last channel with entries before the constant noise signal broke off.

[4] 1, Equ.4, p.4.

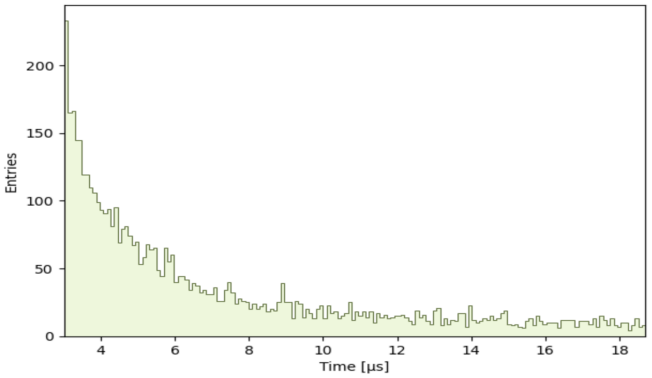

Figure 9. Plot of the converted and rebinned data spectrum

As discussed in I, the data is best modelled using the modified exponential decay law (6).
However knowing that background effects influence the spectrum, the fit function needed a slight modification since it did not consider any noise. We modelled noise as a constant c added to our function, meaning as a constant contribution that is always there. This seems like a reasonable way of modeling noise, since we expect a constant dark current flowing. The fit function then becomes:

$$-\mathrm{d}N(t) = N_{\mu^+} \cdot \left(\frac{1}{f} \cdot \left(\frac{Q}{\tau_\mu} + \Lambda_\mathrm{C}\right) e^{-t(Q/\tau_\mu + \Lambda_\mathrm{C})} + \frac{1}{\tau_\mu} \cdot e^{-t/\tau_\mu}\mathrm{d}t + c \right. \tag{7}$$

where we used (5) to eliminate the τ_eff dependence of the fit function. This means our model has six parameters, 3 of them (Q, Λ_C, f) are fixed values, the other 3 ($\tau_\mu, n = N_{\mu^+}\mathrm{d}t, \mathrm{c}$) starting off at initial parameter values and converging to some other. The values for the fixed parameters were given, and the initial values for the rest were chosen not too small. The plot and values for the relevant parameters emerging from the fit are displayed below:

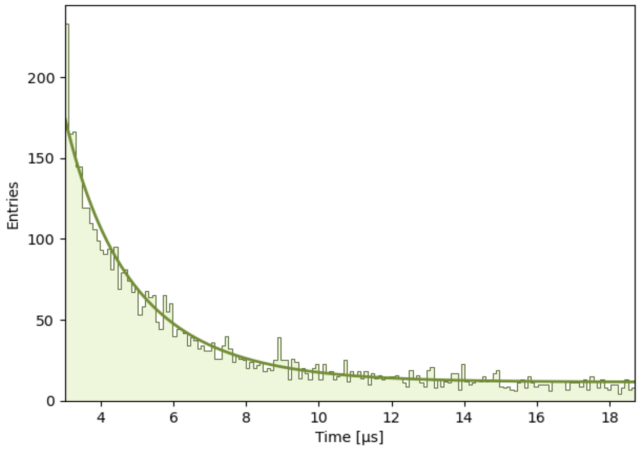

Figure 10. Plot of the fit function overlaying the rebinned data spectrum

Parameter	Value
τ_μ	2.26 ± 0.09 µs
c	11.5 ± 0.05 Entries
χ^2/DoF	1.14286

Table IV. Relevant fit parameters for muon decay function

VI. DISCUSSION

Our result of $\tau_\mu = 2.26 \pm 0.09\,\mu s$ seems to be close to the real value. This is because the fit function fits the data well, which is supported by the value of χ^2/DoF being close to 1. It is also very close to the literature value[5] of $\tau_\mu = 2.19703(4)\mu s$. Therefore it is reasonable to say the experiment was a success.
Our model of constant noise seems to be a good approximation of the actual noise profile, because the fit function fits the data very well across the whole measuring range. Its neccessity can be seen by performing a fit without the parameter c, which yields the result $\tau_\mu = 4.80 \pm 0.07\,\mu s$ with a χ^2/DoF $= 4.38509$, which is not at all within an acceptable range of the literature value[6]. In the plot below, it is also obvious that a fit function of this form does not fit the data very well:

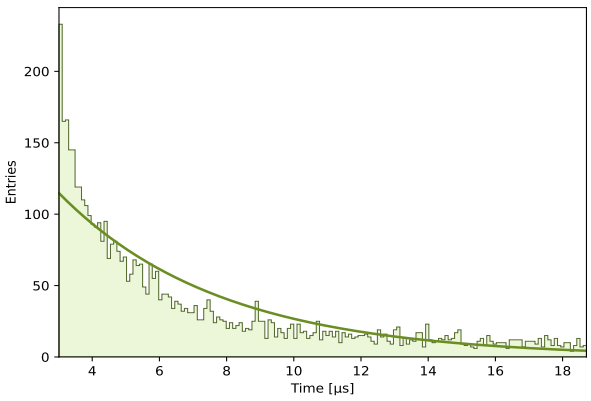

Figure 11. Plot of a fit function without the parameter c overlaying the rebinned data spectrum

It is however still necessary to investigate possible systematic errors of our experimental setup, to further improve the accuracy of our result.

In order to investigate the systematic error caused by uncertainties of the values given for Q and Λ_C for Al[7], the fit was performed again using values for those parameters on both ends of their uncertainty interval. This led to a maximum change of $\tau_\mu + 0.01\,\mu s$, which is well within the calculated uncertainty interval of our result and therefore insignificant.
Another systematic error was introduced by the runtime delay caused by cables and coincidence units. This was already discussed in Section III A and yielded a time delay of $\Delta t = 15.56 \pm 0.32\,ns$. Subtracting this from our result yields an improved value $\tau'_\mu = 2.24 \pm 0.09\,\mu s$. This is even closer to the already mentioned literature value[8], which means this systematic error was significant. Additionally, any error in the time calibration fit will unavoidably alter our conversion from channel number to time. However, looking at the χ^2/DoF value for our linear fit of 0.964444, it can be said that this calibration seems to be very accurate and the assumption of a linear relationship is fulfilled very well.
Other background resulting from noise in the photomultipliers is sufficiently suppressed, as discussed in III B.
During the evaluation of the data, it became clear that choosing optimal starting and ending points for rebinning the measured spectrum was crucial to get accurate results. This was further observed during a test measurement of roughly one hour without the first dual timer and its 3 µs delay. This lead to a very unnatural amount of events within these 3 µs, that we can only assume to be noise.

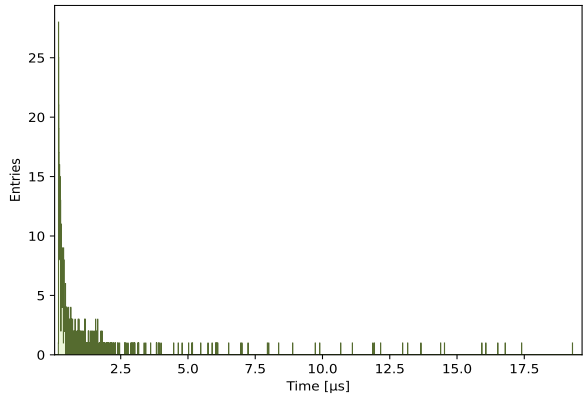

Figure 12. Raw spectrum of a test measurement without the first dual timer

But judging from the accuracy of the fit in Figure (10), our rebinning start and stop values seem to be suited well.

[5] 1, Equ.4, p.4.
[6] 1, Equ.4, p.4.
[7] 1, Table 1, p.5.
[8] 1, Equ.4, p.4.

VII. LITERATURE

l

[1] Dr. Marzieh Bahmani. "Experiment instructions for the advanced internship - Measurement of the muon lifetime". In: *Humboldt-Universität zu Berlin, AG Experimental Elementary Particle Physics* (2023).

[2] David Griffiths. *Introduction to Elementary Particles* - . New York: John Wiley Sons, 2008. ISBN: 978-3-527-61847-7.

[3] William R. Leo. *Techniques for Nuclear and Particle Physics Experiments*. Springer Verlag, 1994.